Resurgence flows in porous media

P. M. Adler*
UPMC Sisyphe., Boîte 105, 4 place Jussieu, 75252 Paris cedex 05, France

V. M. Mityushev†
Department of Mathematics, Pedagogical University, ul. Podchorazych 2, Krakow 30-084, Poland
(Received 8 July 2008; published 18 February 2009)

Porous media with resurgences can be described by a double structure, namely, a continuous porous medium and capillaries with impermeable walls which relate distant points of the continuous medium. The resurgences can be either punctual or extended. The equations for flow in such media are derived; some general properties of the resulting system, which involves nonlocal aspects, are deduced. A "dilute" approximation is detailed for punctual resurgences in two-dimensional media and is illustrated by a few examples.

DOI: 10.1103/PhysRevE.79.026310 PACS number(s): 47.56.+r, 47.63.mf, 91.60.Np

I. INTRODUCTION

Porous media are generally described by the Darcy equation when the length scales are sufficiently large with respect to the pore scale. This approach is also applicable when the media are heterogeneous, i.e., when permeability varies with space, which is the most common case. In addition, real media are very often fractured; for a long time, this complex physical problem has been schematized by the double porosity model devised by [1]. More recently, these fractured media have been addressed directly with a detailed description of the fractures and of their hydrodynamic interaction with the surrounding porous medium [2].

There is another situation that occurs frequently in reservoir studies. One well is connected to a distant well, while it is not connected to closer wells. Such a situation can only be understood if there is a direct link between the two connected wells and if this link has little if any hydrodynamic interaction with the porous medium that it crosses. This link can be a fracture or more likely a set of fractures.

The study of this phenomenon is the main objective of this paper. This phenomenon is called resurgence because of the obvious analogy with rivers which suddenly disappear underground and go out at the ground surface again. Similar ideas have already been developed in two other fields. In physics, random networks limited to nearest neighbors have attracted a lot of attention for a long time; it is only recently that they have been extended to small world models where distant vertices can be related directly by a link [3]. The electrical testing of porous media by electrical probes located at the walls is called electrical tomography and has been used frequently in geophysics since it is a noninvasive technique; a series of electrodes are placed on a wall; two of them are used to inject the current and the resulting potential differences are measured at the others (see [4] for a recent application). The distribution of the resistivities inside the material can be derived by inverting the measurements which requires the resolution of the Laplace equation. It is interesting to note that this classical technique corresponds exactly to the situation that we wish to address from a different perspective.

Media with resurgences consist of a double structure. The first one, which is continuous, is described by Darcy law as usual. The second one models the resurgences by capillaries with impermeable walls, which relate distant points of the continuous medium.

These two structures have already been studied separately in previous works. Networks were addressed by graph theory in [5–8] and extensive literature has been devoted to studies of porous media on the Darcy scale (see [6,9], and the literature cited therein).

This double structure is assumed to be spatially periodic; therefore, the theory of homogenization (see, for instance, [10]) will be used to determine the macroscopic quantities. Since this first paper is restricted to two-dimensional periodic problems, the methods developed for the determination of the effective conductivity can be applied [11–16].

This paper is organized as follows. A simple physical presentation and elementary solutions are given in Sec. II for one-dimensional structures. The full problem is presented in Sec. III as the superposition of a network and of a continuous medium; it involves some nonlocal aspects when the resurgences are extended.

The rest of the paper is devoted to punctual resurgences. In Sec. IV, the total macroscopic permeability is introduced. It is calculated by means of a conjugation (transmission) problem for circular multiply connected domains in Sec. V. The method of complex potentials is applied in Sec. V B to obtain constructive formulas in Sec. V C for the total macroscopic permeability in terms of the flow rates inside the capillaries.

Section VI is devoted to the solution of the two-scale problem by combining and developing the methods presented in [5,6,13–15]. The network and the continuous phases of the problem are connected by the unknown flow rates along the capillaries j_m. In Sec. VI A, the continuous problem is partially solved in the zeroth approximation. More precisely, the pressures at both ends of the capillaries are expressed by the unknown j_m. Then, these relations are used in Sec. VI B to solve the closed network problem and to determine j_m. In Sec. VI C, the problem is completely solved

*pierre.adler@upmc.fr
†vmityu@yahoo.com

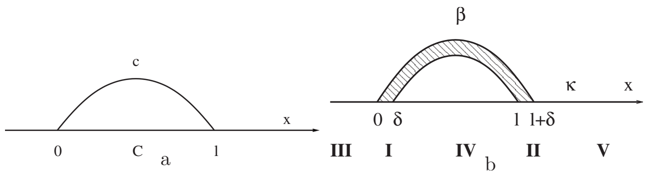

FIG. 1. One-dimensional medium. (a) Punctual resurgence. (b) Extended resurgence.

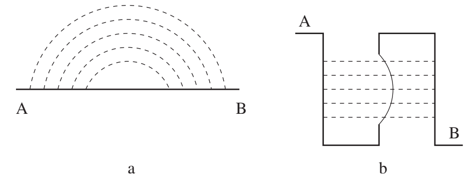

FIG. 2. Two possible configurations for extended one-dimensional resurgences. The symmetric and antisymmetric cases (a) and (b) correspond to Eqs. (2.6a) and (2.6b), respectively. The solid line AB corresponds to the x axis of Fig. 1; the broken lines schematize the resurgences. In (b), the central part of the x axis (represented by the thin solid arc) is continuous, but does not intersect the resurgences.

under the assumption that the radii of the capillaries are small when compared to the distances between the ends of any two capillaries. As a result, Eq. (6.33) is derived for the total macroscopic permeability, which for usual continuous media without networks, yields the famous Clausius-Mossotti approximation [17]. Section VII contains two applications of the general formulas.

The Appendix contains a proof of a formula for the seepage velocity. It differs from the classical formula [18], which expresses the equality of the permeability calculated by the spatial averaging over the unit cell and by the balance of the input and output volumes of fluid in the unit cell.

II. ONE-DIMENSIONAL GENERAL PROBLEM

One-dimensional stationary problems provide the opportunity to illustrate resurgence flows in a simple way without any general and heavy mathematical apparatus. Two cases can be distinguished depending on whether the resurgences are punctual or extended as illustrated in Fig. 1. A known pressure gradient $\frac{dp}{dx}|_\infty$ is acting at infinity along the x axis on these two configurations.

A. Punctual resurgences

This problem is elementary since it corresponds to two parallel capillaries; it is detailed to introduce some notations. Along a finite capillary, the flow rate j is related to the pressure gradient dp/dx by the general equation

$$j = -\frac{c}{\mu}\frac{dp}{dx}, \tag{2.1}$$

where μ is the fluid viscosity and c is the conductivity homogeneous to a length at the power 4. Let us assume that the conductivities of the infinite and finite capillaries in Fig. 1(a) are equal to C and c, respectively. The pressure gradient at $x = \pm\infty$ is equal to $dp/dx|_\infty$. The flow rates J and J_L along the infinite capillary are given by

$$J = -\frac{C}{\mu}\left.\frac{dp}{dx}\right|_\infty, \quad x < 0 \text{ and } x > l, \tag{2.2}$$

$$J_L = -\frac{C}{\mu}\frac{[p(l) - p(0)]}{l} \quad \text{for } 0 < x < l.$$

In a similar way, the flow rate j in the small capillary is

$$j = -\frac{c}{\mu}\frac{[p(l) - p(0)]}{l_c}, \tag{2.3}$$

where l_c is the length of the small capillary. The pressure difference $p(l) - p(0)$ can be determined by equating $J_L + j$ to J,

$$p(l) - p(0) = \left(1 + \frac{c}{C}\frac{l}{l_c}\right)^{-1} l \left.\frac{dp}{dx}\right|_\infty, \tag{2.4}$$

from which all the quantities can be derived.

B. Extended resurgences

Now the situation is slightly different and is illustrated in Fig. 1(b). The x axis can be divided into five parts. Parts III, IV, and V are classical capillaries with conductivity κ and Eq. (2.1) can be replaced by the one-dimensional Laplace equation

$$\frac{d^2p}{dx^2} = 0. \tag{2.5}$$

The two segments I and II are related by an extended resurgence of conductance β, which is composed of parallel capillaries that do not exchange mass with each other. This corresponds physically to a series of parallel fractures separated by impermeable rocks. Such a situation is frequently observed in the field; a recent illustration was given by [19].

This situation, which is illustrated in Fig. 1(b), modeled as follows. At each point $x \in [0, \delta]$, there exists a resurgence capillary whose end is at $l + \delta - x \in [l, \delta + l]$. The flow rate going from x to $l + \delta - x$ along this capillary is equal to

$$\frac{\beta}{\mu}[p(x) - p(l + \delta - x)]d^2x, \tag{2.6a}$$

where β is some positive constant. This is schematized in Fig. 2(a). For obvious reasons, this case is called symmetric.

A more interesting possibility is illustrated in Fig. 2(b). Now, the flow rate goes from x to $x + l$ and is equal to

$$\frac{\beta}{\mu}[p(x) - p(x + l)]d^2x. \tag{2.6b}$$

This is called the antisymmetric case.

Let us detail this latter case since it is not classical; a mass balance along the x axis between the points x and $x+dx$ yields

$$-\frac{\kappa}{\mu}dp(x) = -\frac{\kappa}{\mu}dp(x+dx) + \frac{\beta}{\mu}[p(x)-p(x+l)]d^2x. \tag{2.7}$$

Therefore,

$$\frac{\kappa}{\mu}\frac{d^2p}{dx^2} + \frac{\beta}{\mu}[p(x+l)-p(x)] = 0 \quad \text{for } 0 < x < \delta. \tag{2.8a}$$

A similar equation holds for $x \in [l, l+\delta]$

$$\frac{\kappa}{\mu}\frac{d^2p}{dx^2} + \frac{\beta}{\mu}[p(x-l)-p(x)] = 0 \quad \text{for } l < x < l+\delta. \tag{2.8b}$$

These equations can be simplified by introducing the dimensionless quantities

$$x = x'l, \quad \alpha = \frac{\beta l^2}{\kappa}. \tag{2.9}$$

For simplicity, the usual notations without primes are used in the rest of this section. Note that β is positive so that fluid flows from higher to lower pressures.

Equation (2.5) can be readily integrated in domains III, IV, and V. The solution is unique within an arbitrary constant, which can be taken equal to 0,

$$p(x) = ax \text{ in III}, \quad p(x) = bx + d \text{ in IV}, \quad p(x) = ax + e \text{ in V}, \tag{2.10}$$

where b, d, and e are unknown constants; the constant a is equal to $a = dp/dx|_\infty$.

The differential-difference equations (2.8a) and (2.8b) can be reduced to a system of ordinary differential equations by introducing

$$q(x) = p(x+l) \quad \text{for } 0 < x < \delta. \tag{2.11}$$

By adding Eqs. (2.8a) and (2.8b), it is easily seen that the second derivative of $p+q$ is equal to 0. Therefore,

$$q(x) = -p(x) + c_1x + c_2 \quad \text{for } 0 < x < \delta, \tag{2.12}$$

where c_1 and c_2 are two constants. Using Eq. (2.11), substitute Eq. (2.12) into Eq. (2.8b) when expressed in terms of p to obtain

$$\frac{d^2p}{dx^2} + \alpha[-2p(x) + c_1x + c_2] = 0 \quad \text{for } 0 < x < \delta. \tag{2.13}$$

This ordinary differential equation has the general solution

$$p(x) = \tfrac{1}{2}(c_1x + c_2) + c_3\exp(\sqrt{2\alpha}x) + c_4\exp(-\sqrt{2\alpha}x) \quad \text{for } 0 < x < \delta, \tag{2.14}$$

where c_3 and c_4 are arbitrary constants. Analogously,

$$p(x) = \tfrac{1}{2}[c_1(x-l) + c_2] + c_3\exp[\sqrt{2\alpha}(x-l)] + c_4\exp[-\sqrt{2\alpha}(x-l)] \quad \text{for } l < x < l+\delta. \tag{2.15}$$

The boundary conditions are the following. The pressure gradient a at $x=\pm\infty$ is equal to the imposed pressure gradient $dp/dx|_\infty$. Moreover, the pressure and the flow rates should be continuous. Therefore, the continuity condition should be satisfied at $x=0$, δ, l, $l+\delta$; the last condition at $x=l+\delta$ is redundant since the flow rates are conserved both along the x axis and the resurgence.

Hence, seven equations can be written down for the seven unknowns b, d, e, c_1, c_2, c_3, and c_4. These constants can be found from the corresponding system of linear algebraic equations. In addition, the determinant of the system can be calculated as

$$\sqrt{2}[1+\exp(\sqrt{2\alpha}\delta)] + [\exp(\sqrt{2\alpha}\delta) - 1]\sqrt{\alpha}(2l-\delta). \tag{2.16}$$

It is seen to always be positive.

Similar developments can be made for the symmetric case (2.6a). Systematic results are shown in Fig. 3 for $l=10$. Four values of δ were investigated, namely, 0.1, 0.5, 1, and 2 as well as four values of α equal to 1, 1.5, 3, and 10. The pressure drop at infinity is equal to -1 and the fluid is expected to flow from left to right. The results are classical in the sense that pressure decreases everywhere with x; moreover, the roles of β and κ follow the physical expectations.

The same calculations were done for the antisymmetric case (2.6b) and results are displayed in Fig. 4 for the same set of parameters as in Fig. 3. When the width δ of the resurgence is small, the evolution of the pressure along the x axis is classical as observed in Fig. 4(a); it constantly de-

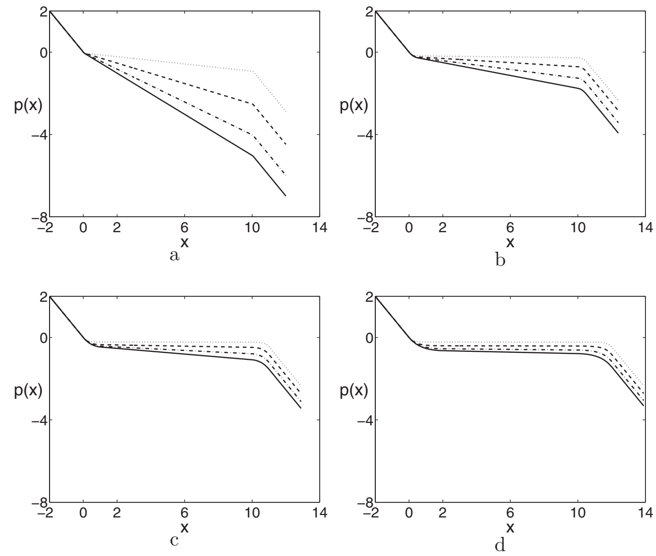

FIG. 3. Pressure $p(x)$ along the x axis for an extended one-dimensional symmetric resurgence described by Eq. (2.6a) and illustrated in Fig. 2(a). Data are for $\frac{dp}{dx}|_\infty=-1$, $l=10$. $\delta=0.1$ (a), 0.5 (b), 1 (c), and 2 (d). In each subfigure, $\alpha=1$ (solid line), 1.5 (dashed-dotted line), 3 (dashed), and 10 (dotted).

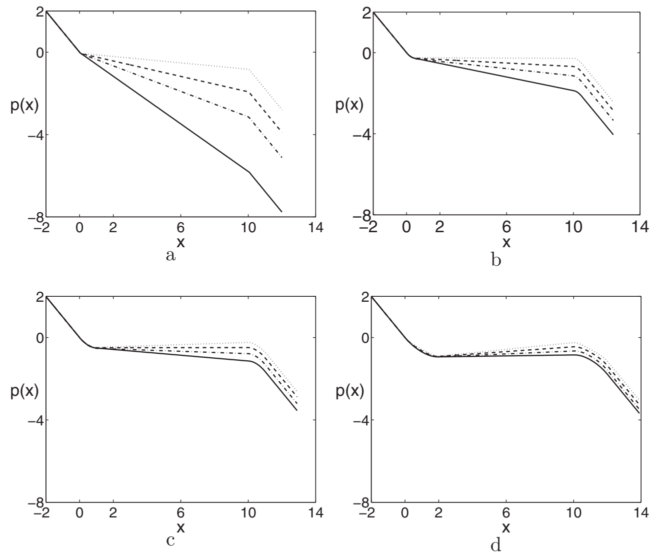

FIG. 4. Pressure $p(x)$ along the x axis for an extended one-dimensional antisymmetric resurgence described by Eq. (2.6b) and illustrated in Fig. 2(b). Conventions are the same as in Fig. 3.

creases and the pressure drop $|\Delta p|_1^l$ between $x=\delta$ and l decreases with α since the flow rate along the x axis is expected to decrease.

However, when δ and α increase, the pressure gradient between $x=\delta$ and l becomes negative, which means that the fluid flows from right to left between these two points along the infinite capillary. This behavior seemed to be unphysical and the calculations were done in two different ways to be sure of the results. Actually, a closer look at the numerical data shows that when α is large, most of the fluid flows through the resurgence; $p(x)$ is always larger than $p(x+l)$ $(0<x<\delta)$, which means that the fluid flows from left to right as it should inside the resurgence capillaries. However, along the x axis, the direction of the flow is imposed by the difference $p(x=\delta)-p(x=l)$; for large values of δ and of α, this difference is negative, which implies that the fluid flows from right to left between δ and l along the x axis.

Therefore, this back flow is expected to occur when resurgence flow is important; it is exactly what is observed in Fig. 4. Even this elementary one-dimensional situation displays an interesting behavior.

Two additional remarks can be made on this phenomenon. First, it seems crucial that the resurgence capillaries go from x to $x+l$ in this order. With the choice (2.6a) where the resurgence capillaries would go from x to $l+\delta-x$ for $x\in[0,\delta]$, it is obvious that there cannot be any back flow.

Second, it is essential that both δ and α are large. If one of these parameters is not sufficiently large, the system follows a classical behavior.

III. STATEMENT OF THE PROBLEM

A. General

The general equations, which govern resurgence flows in porous media, are presented in this section. The medium is assumed to be composed of a capillary network and of a continuous medium, which are connected at some vertices of the network as it is schematized in Fig. 5.

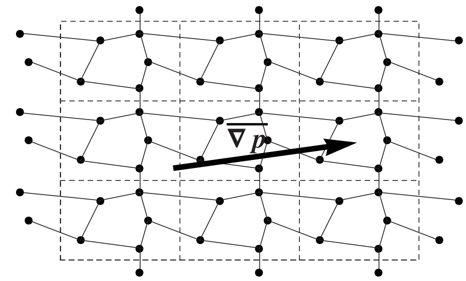

FIG. 5. A doubly periodic graph energized by a macroscopic pressure gradient $\overline{\nabla p}$.

An overview of the main equations can be given in this section. Note that all the dimensional and the dimensionless quantities are noted with and without a prime, respectively. A macroscopic pressure gradient $\overline{\nabla' p'}$ is imposed on this medium. Let ℓ' be a characteristic length. These two quantities can be used to define a unit pressure $\mathcal{P}$,

$$\mathcal{P}=\ell'|\overline{\nabla' p'}|. \tag{3.1}$$

Fluid flows through the continuum and through the capillaries. The local velocity $\mathbf{v}_c'$ through the continuous medium obeys the classical Darcy equation

$$\mathbf{v}_c'=-\frac{\mathbf{K}'}{\mu'}\cdot\overline{\nabla' p'}. \tag{3.2}$$

The flow rate J_k' through the capillary k is of the form (2.3),

$$J_k'=\frac{\alpha_k'}{\mu'}[p'(\mathbf{R}_{k-}')-p'(\mathbf{R}_{k+}')], \tag{3.3}$$

where the capillary is oriented from $\mathbf{R}_{k-}'$ to $\mathbf{R}_{k+}'$. $\mathbf{K}'$ and α_k' are homogeneous to the square and to the cube of a length, respectively.

There are two major possibilities to choose the length and time scales ℓ' and T'. They can be based on the flow in the porous medium (3.2),

$$T'=T_c'=\frac{\mu'}{K'|\overline{\nabla' p'}|},\quad \ell'=\ell_c'=\sqrt{K'}, \tag{3.4}$$

or they can be based on the network flow rates

$$T'=T_n'=\frac{\mu'\ell'^2}{\alpha'|\overline{\nabla' p'}|},\quad \ell'=\ell_n'=r', \tag{3.5}$$

where r' is a typical capillary radius.

At this level of generality, it will not be chosen between these possibilities. Two dimensionless parameters are naturally introduced in the problem

$$A=\frac{\sqrt{K'}}{r'},\quad B=\frac{\ell'}{\sqrt{\ell_1'\ell_2'}}, \tag{3.6}$$

where ℓ_1' and ℓ_2' are the lateral dimensions of the unit cell.

The relations between the main dimensional (primed) quantities and their dimensionless counterparts can be summarized by

$$\mathbf{x}' = \ell'\mathbf{x}, \quad t' = T't, \quad \mathbf{v}' = \frac{\ell'}{T'}\mathbf{v}, \quad J' = \frac{\ell'^2}{T'}J, \quad p' = \mathcal{P}p. \tag{3.7}$$

Finally, the area $\mathcal{S}'$ of the unit cell is given by

$$\mathcal{S}' = \ell_1'\ell_2' = \ell'^2\mathcal{S}. \tag{3.8}$$

Let a two-dimensional (2D) rectangular lattice be generated by the dimensionless translation vectors

$$\mathbf{R_m} = m_1\mathbf{i}_1 + m_2\mathbf{i}_2, \tag{3.9}$$

where $\mathbf{i}_1$ and $\mathbf{i}_2$ are the fundamental translation vectors, m_1 and m_2 are integers and $\mathbf{m}=(m_1,m_2)$ is the corresponding vector. Consider the unit cell

$$\mathcal{Q}_0 = \left\{\mathbf{x} = t_1\mathbf{i}_1 + t_2\mathbf{i}_2 \in \mathbb{R}^2 : -\tfrac{1}{2} < t_{1,2} < \tfrac{1}{2}\right\}. \tag{3.10}$$

Each cell is obtained from $\mathcal{Q}_0$ by a translation

$$\mathcal{Q} = \mathcal{Q}_0 + \mathbf{R_m}. \tag{3.11}$$

The vector $\mathbf{i}_1$ is directed along the x axis and the second coordinate of $\mathbf{i}_2$ is positive. For simplicity, it is assumed that the cell $\mathcal{Q}_0$ is rectangular; hence, the fundamental translation vectors can be written as

$$\mathbf{i}_1 = (\ell_1,0), \quad \mathbf{i}_2 = (0,\ell_2), \tag{3.12}$$

with $\mathcal{S}=\ell_1\ell_2$.

B. Network problem

Let $\mathbf{a}_m$ $(m=1,2,\ldots,N)$ be points which belong to $\mathcal{Q}_0$. A periodic network involving $\mathbf{a}_m+\mathbf{R_m}$ can be treated as a doubly periodic graph, i.e., as a graph which is periodic along two independent spatial directions. This graph can be presented as a finite graph with vertices at $\mathbf{a}_m$ $(m=1,2,\ldots,N)$ on the torus derived from the unit cell $\mathcal{Q}_0$ by identifying the opposite sides of $\mathcal{Q}_0$. Such graphs are called local graphs (see Fig. 6).

Following [5,6], some notations are introduced for the local graph Γ. Let $V\Gamma=\{\mathbf{a}_m, m=1,2,\ldots,N\}$ and $E\Gamma=\{e_k, k=1,2,\ldots,M\}$ denote the sets of vertices (or junctions) and of edges (or links) of Γ. The vertices $\mathbf{a}_m+\mathbf{R_m}$ are said to be homologous to $\mathbf{a}_m \in V\Gamma$. Choose an arbitrary orientation for the edges, and define a scalar flow rate J_k along the edge e_k. These orientations are used to define a $N\times M$ incident matrix $\mathbf{D}$. D_{ij} is equal to 1 if the edge j arrives on the vertex i, and to -1 in the opposite case. D_{ij} is equal to zero if j does not start or end at i. The sum of each row of $\mathbf{D}$ is obviously equal to zero and the rank of $\mathbf{D}$ is $N-1$.

A cycle Q of Γ can be represented by the cycle vector ξ_Q defined as follows. $\xi_Q(e_k)$ is equal to 1 if e_k belongs to Q and if its orientation in Q coincides with its orientation in Γ. $\xi_Q(e_k)$ is equal to -1 if e_k belongs to Q and if its orientation in Q is opposite to its orientation in Γ. $\xi_Q(e_k)$ is equal to 0 if e_k does not belong to Q. Every cycle vector $\xi_Q\Gamma$ verifies

$$\mathbf{D}\cdot\xi_Q = \mathbf{0}. \tag{3.13}$$

The set of cycles of Γ generates a subspace of $E\Gamma$ whose dimension is $M-N+1$ [5,6]. Let $\mathbf{C}$ be the $M\times(M-N+1)$ matrix whose kth column is the fundamental cycle vector ξ_Q. The rank of $\mathbf{C}$ is $M-N+1$; the N independent equations of Eq. (3.13) can be summarized by

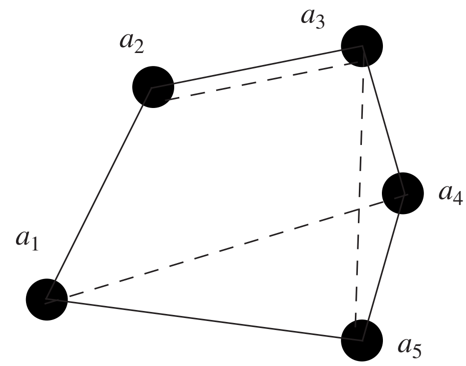

FIG. 6. The local graph in the unit cell $\mathcal{Q}_0$ of the periodic graph presented in Fig. 5. The edge space $E\Gamma$ is composed of the eight solid and broken lines, which relate the five vertices a_m $(m=1,\ldots,5)$; the solid lines correspond to the edges within the periodicity cell and the dashed lines correspond to the edges connecting vertices which lie in adjacent cells. A possible spanning tree T is composed by the four successive edges which relate a_1-a_2-a_3-a_4-a_5. The chords of T are the three broken lines to which should be added the edge a_1-a_5.

$$\mathbf{D}\cdot\mathbf{C} = \mathbf{0}. \tag{3.14}$$

A spanning tree T is a set of connected edges which relate all the vertices of a graph, but which contains no cycle. A chord of T is an edge which does not belong to T. Independent cycles may be deduced from any spanning tree T of the graph Γ. To each chord of T may be associated a unique cycle whose extra elements are contained in T. The edges of Γ are labeled in such a way that the first $N-1$ edges $e_1,e_2,\ldots,e_{N-1}$ belong to T and that $e_N,e_{N+1},\ldots,e_M$ are the chords of T. All these definitions are illustrated in Fig. 6.

The edge space $E\Gamma$ can be decomposed into $E_T\oplus E_S$, where E_T and E_S are the subspaces spanned by the tree edges and the chords, respectively. $\mathbf{D}$ and $\mathbf{C}$ may be represented as

$$\mathbf{D} = \begin{pmatrix} \mathbf{D}_T & \mathbf{D}_S \\ & \mathbf{d}_N \end{pmatrix}, \quad \mathbf{C} = \begin{pmatrix} \mathbf{C}_T \\ \mathbf{I}_{M-N+1} \end{pmatrix}, \tag{3.15}$$

where $\mathbf{I}_{M-N+1}$ is the unit matrix of dimension $M-N+1$. Since T is a spanning tree, $\mathbf{D}_T$ is nonsingular and the last line $\mathbf{d}_N$ is linearly dependent on the other lines of $\mathbf{D}$. The matrix $\mathbf{C}_T$ can be determined by $\mathbf{D}_T$ and $\mathbf{D}_S$ [5,6],

$$\mathbf{C}_T = -\mathbf{D}_T^{-1}\cdot\mathbf{D}_S. \tag{3.16}$$

A pressure may be assigned to each vertex of the network, say $p_m(\mathbf{a}_m+\mathbf{R_m})$, where $\mathbf{R_m}$ is given by Eq. (3.9). The periodicity of the local pressure gradient permits the local pressure to be decomposed into the sum

$$p_m(\mathbf{a}_m+\mathbf{R_m}) = p_m + \mathbf{R_m}\cdot\overline{\boldsymbol{\nabla}p}, \tag{3.17}$$

where p_m is the pressure at $\mathbf{a}_m$.

The flow rate J_k between two adjacent vertices accompanying the Stokes flow is proportional to the pressure drop between these vertices,

$$J_k = \alpha_k[p_m(\mathbf{a}_m + \mathbf{R_m}) - p_{m'}(\mathbf{a}_{m'} + \mathbf{R}_{\mathbf{m}'})], \qquad (3.18)$$

where the edge e_k joins the vertex $\mathbf{a}_m$ to the vertex $\mathbf{a}_{m'}$, which belongs to the cell $\mathbf{R}_{\mathbf{m}'}$. Here, α_k ($k=1,\ldots,M$) are positive constants. The homology group of the torus is taken into account in Eq. (3.18). It can be detailed by the example given in Fig. 6.

The total flux should be conserved at each vertex; therefore,

$$\sum_{k\in\Omega^+(m)} J_k - \sum_{k\in\Omega^-(m)} J_k = j_m, \quad m=1,2,\ldots,N, \quad (3.19)$$

where $\Omega^{\pm}(m)$ correspond to the edges ending and beginning at the vertex $\mathbf{a}_m$, respectively; j_m denotes the flow rate at $\mathbf{a}_m$, i.e., the flow rate passing through $\mathbf{a}_m$ into the continuous medium with the adequate sign (fluid flows out of the network if j_m is positive and into it in the opposite case). Thus, the sign of j_m does not depend on the orientation of the graph Γ in contrast with the sign of J_k. Substitution of Eq. (3.18) into Eq. (3.19) yields

$$\sum_{k\in\Omega^+(m)} \alpha_k[p_{m'}(\mathbf{a}_{m'} + \mathbf{R}_{\mathbf{m}'}) - p_m] - \sum_{k\in\Omega^-(m)} \alpha_k[p_m - p_{m'}(\mathbf{a}_{m'} + \mathbf{R}_{\mathbf{m}'})] = j_m,$$
$$m=1,2,\ldots,N. \qquad (3.20)$$

Let $\Omega(m)=\Omega^+(m)\cup\Omega^-(m)$. Then Eq. (3.20) becomes

$$\sum_{k\in\Omega(m)} \alpha_k[p_m - p_{m'}(\mathbf{a}_{m'} + \mathbf{R}_{\mathbf{m}'})] = -j_m, \quad m=1,2,\ldots,N. \qquad (3.21)$$

Here, only the pressures p_m at the vertices $\mathbf{a}_m$ in the cell $\mathcal{Q}_0$ are taken into account.

In the network problem, it is necessary to derive p_m and J_k from Eqs. (3.17) and (3.21). This is possible if $(j_m; m=1,2,\ldots,N)$ is known. The continuous problem should be solved in order to provide the missing equations for j_m.

C. Continuous problem

Consider the continuous medium when the vertices $\mathbf{a}_m$ are replaced by the nonoverlapping simply connected domains D_m with the smooth boundaries ∂D_m oriented counterclockwise. Let D be the complementary of the unit cell (3.10) to all domains D_m in the topology of the torus introduced in Sec. III B. The flow in the porous medium is governed by the Darcy equation in the domain D,

$$\mathbf{v} = -\mathbf{K}\cdot\nabla p, \quad \nabla\cdot\mathbf{v} = 0, \qquad (3.22)$$

where $\mathbf{v}$ denotes the local seepage velocity, $\mathbf{K}$ is the permeability tensor, and ∇p is the local pressure gradient. The pressure gradient is spatially periodic and the pressure field verifies

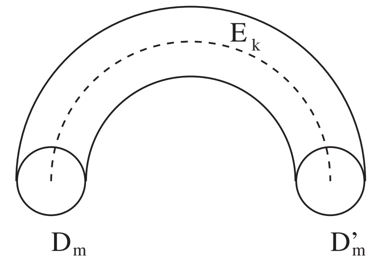

FIG. 7. A capillary E_k and its network approximation by the edge e_k (dashed line).

$$p(\mathbf{x} + \mathbf{R_m}) = p(\mathbf{x}) + \mathbf{R_m}\cdot\overline{\nabla p}. \qquad (3.23)$$

The flow rate j_m at $\mathbf{a}_m$ in the continuous medium is defined as the volume of fluid passing through ∂D_m,

$$j_m = \int_{\partial D_m} d\lambda\, \mathbf{n}\cdot\mathbf{v}, \quad m=1,2,\ldots,N, \qquad (3.24)$$

where $\mathbf{n}$ stands for the outward normal vector to ∂D_m and $d\lambda$ for the dimensionless length element.

The pressure p satisfies an elliptic equation in D,

$$\nabla\cdot(\mathbf{K}\cdot\nabla p) = 0. \qquad (3.25)$$

Equation (3.24) can be written via the generalized normal derivative of the pressure as

$$j_m = -\int_{\partial D_m} d\lambda\, \mathbf{n}\cdot\mathbf{K}\cdot\nabla p, \quad m=1,2,\ldots,N. \quad (3.26)$$

In order to match the continuum with the network, a capillary is considered as a channel E_k connecting two domains D_m and D'_m (see Fig. 7). The capillaries E_k are assumed to lie out of the plane where the continuous flow takes place. The length and the width of E_k are denoted by L_k and r_k, respectively. These two quantities are assumed to verify

$$r_k \ll L_k. \qquad (3.27)$$

Then, the flow in E_k can be described as a Poiseuille flow in the tube E_k with the averaged pressures p_m and p'_m over D_m and D'_m, respectively, and the nonslip condition on the other part of the boundary of E_k. The total flow in the medium can be considered as a two-scale flow in E_k and in D as follows. The flow in E_k is approximated by a one-dimensional (1D) flow along the edge e_k by Eqs. (3.18)–(3.21) with appropriate coefficients α_k. Simultaneously, the flow in D is described by Eq. (3.22). The point conditions (3.21) are replaced by continuous conditions having the same form, but with another interpretation of p_m. It is assumed that the pressure p is constant and equal to p_m at ∂D_m. Therefore,

$$p(\mathbf{x}) = p_m, \quad \mathbf{x}\in\partial D_m, \quad m=1,2,\ldots,N. \qquad (3.28)$$

Using Eqs. (3.26) and (3.28), the continuous condition (3.21) can be written as

$$\sum_{k\in\Omega(m)} \alpha_k[p_m - p_{m'}(\mathbf{a}_{m'} + \mathbf{R}_{\mathbf{m}'})] = \int_{\partial D_m} d\lambda \mathbf{n}\cdot\mathbf{K}\cdot\nabla p, \quad m=1,2,\ldots,N, \qquad (3.29)$$

where $p_{m'}(\mathbf{a}_{m'}+\mathbf{R}_{\mathbf{m}'})$ is expressed in terms of $p_{m'}$ by Eq. (3.17).

Thus, the following boundary value problem is obtained. The field $p(\mathbf{x})$ obeys Eq. (3.25) in D, is continuously differentiable in the closure of D, and satisfies the quasiperiodic relations (3.23), the boundary conditions (3.28) and (3.29). The constants p_m $(m=1,2,\ldots,N)$ have to be determined after this problem is solved.

The stated problem is closed. It is not purely continuous since the problem contains the flow on the graph corresponding to the left-hand side of Eq. (3.29). One can see that Eq. (3.29) relates the generalized normal derivative of p and the values of p on different parts of the boundary. This makes the problem nonlocal, in contrast with the classical boundary value problems. It is worth noting that the relations (3.21) and (3.29) do not depend on the choice of the orientation of the graph Γ.

In the limit case $\alpha_k=0$, Eq. (3.29) becomes

$$\int_{\partial D_m} d\lambda \mathbf{n}\cdot\mathbf{K}\cdot\nabla p = 0, \quad m=1,2,\ldots,N. \qquad (3.30)$$

Then, a modified Dirichlet problem (3.28) is derived with the undetermined constants p_m and the additional conditions (3.30) (see [13]).

The relations (3.28) and (3.29) provide a simplified picture for the flow near D_m, which is described by the two constants p_m and j_m. In extended resurgences, boundary conditions are needed to describe the flow near D_m more precisely. Let F_k: $D_m \to D_{m'}$ denote a diffeomorphism (i.e., a bijective differentiable transformation) between D_m and $D_{m'}$ corresponding to the edge $e_k \in V\Gamma$; note that this transformation is defined whatever the orientation of the edge e_k. Hence, F_k summarizes the transport properties of e_k described by Eq. (3.18) in the previous version of the problem. $F_k(\mathbf{x})$ is assumed to be equal to $\mathbf{x}+\mathbf{R}_{\mathbf{m}}$ when it relates homologous domains D_m and $D_{m'}$ with $D_{m'}=D_m+\mathbf{R}_{\mathbf{m}}$. The problem is periodic with period $\mathbf{R}_{\mathbf{m}}$ and Eqs. (3.28) and (3.29) can be replaced by the more general conditions

$$\nabla\cdot[\mathbf{K}\cdot\nabla p(\mathbf{x})] - \sum_{k\in\Omega(m)} \alpha_k[p(\mathbf{x}) - p(F_k(\mathbf{x}))] = 0, \quad \mathbf{x}\in D_m. \qquad (3.31)$$

In physical terms, F_k corresponds to the extended resurgences defined in Sec. II B. These resurgences can be within a single unit cell or relate two different unit cells.

In the present paper, most of the attention is paid to condition (3.29) for locally isotropic continuous media when $\mathbf{K}(\mathbf{x})=K\mathbf{I}$. If the scalar permeability K is assumed to be constant in D, Eq. (3.25) is reduced to the Laplace equation

$$\nabla^2 p = 0. \qquad (3.32)$$

In this case, Eq. (3.29) can be simplified as

$$\sum_{k\in\Omega(m)} \alpha_k[p_m - p_{m'}(\mathbf{a}_{m'} + \mathbf{R}'_{\mathbf{m}})] = K\int_{\partial D_m} \frac{\partial p}{\partial \mathbf{n}} d\lambda, \quad m=1,2,\ldots,N. \qquad (3.33)$$

Equation (3.26) becomes

$$j_m = -K\int_{\partial D_m} \frac{\partial p}{\partial \mathbf{n}} d\lambda, \quad m=1,2,\ldots,N. \qquad (3.34)$$

Summation of Eqs. (3.34) and the fact that the integral of the normal derivative of a harmonic function over the boundary vanishes yield the relation

$$\sum_{m=1}^{N} j_m = 0. \qquad (3.35)$$

This property can also be proved by considering only the network. Since the fluid is incompressible, the total flow rate $\Sigma_{m=1}^{N} j_m$ entering the network is necessarily equal to 0.

IV. MACROSCOPIC TOTAL PERMEABILITY

Consider the seepage velocity $\mathbf{v}_c=(v_x,v_y)$ in the cell $\mathcal{Q}_0$ and the velocity $\mathbf{v}_n$ in the capillaries E_k $(k=1,2,\ldots,M)$ with the linear sizes r_k and L_k satisfying Eq. (3.27). The average total velocity in the medium is defined as the integral over the continuous medium D plus the integral over the capillaries in application of the general definition (A2a),

$$\overline{\mathbf{v}} = \mathcal{S}^{-1}\left[\int_D \mathbf{v}_c d\mathbf{x} + \int_V \mathbf{v}_n d\mathbf{x}\right]. \qquad (4.1)$$

The three-dimensional derivation is detailed in the Appendix. $\overline{\mathbf{v}}$ can be written as

$$\overline{\mathbf{v}} = \mathcal{S}^{-1}\left[\int_{\partial\mathcal{Q}_0} \mathbf{x} d\lambda \mathbf{n}\cdot\mathbf{v} + \sum_{k=1}^{M}\mathbf{R}(k)J_k\right], \qquad (4.2)$$

where $\mathbf{R}(k)$ is the macroscopic jump associated with the edge $e_k \in E\Gamma$ and J_k is the flow rate (3.18). Here, the flow in the spatial capillary E_k is approximated by the flow in the edge e_k of the graph Γ.

The total dimensionless permeability tensor $\overline{\mathbf{K}}$ is defined by means of the dimensionless macroscopic Darcy law

$$\overline{\mathbf{v}} = -\overline{\mathbf{K}}\cdot\overline{\nabla p}, \qquad (4.3)$$

with the obvious decomposition into the continuous and the network contributions

$$\overline{\mathbf{K}} = \overline{\mathbf{K}_c} + \overline{\mathbf{K}_n}. \qquad (4.4)$$

In order to derive a compact expression for $\overline{\mathbf{K}}$, it is usual [6] to introduce higher order vectors and tensors by

$$p(\mathbf{x}) = \mathcal{P}(\mathbf{x})\cdot\overline{\nabla p}, \quad J_k = \mathcal{J}_k\cdot\overline{\nabla p}, \quad \mathbf{v}(\mathbf{x}) = \mathcal{V}(\mathbf{x})\cdot\overline{\nabla p}, \qquad (4.5)$$

where $\mathcal{P}(\mathbf{x})$ and $\mathcal{J}_k$ are vectors while $\mathcal{V}(\mathbf{x})$ is a second order tensor. Then, it is an easy matter to introduce these defini-

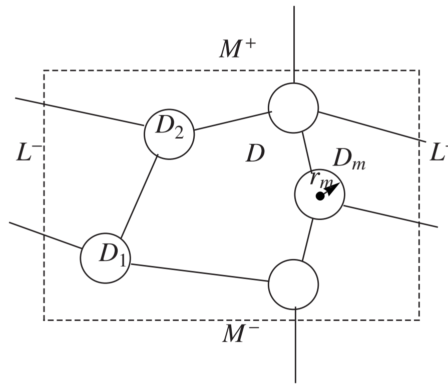

FIG. 8. The unit cell with disks corresponding to Fig. 6.

tions into Eq. (4.2) and to obtain by comparison with Eq. (4.3),

$$\bar{\mathbf{K}} = -\mathcal{S}^{-1}\left[\int_{\partial Q_0} \mathbf{x} d\lambda \mathbf{n}\cdot\mathcal{V} - \sum_{k=1}^{M}\mathbf{R}(k)\mathcal{J}_k\right]. \tag{4.6}$$

The vectors

$$\mathcal{P} = (\mathcal{P}^{(1)}(\mathbf{x}), \mathcal{P}^{(2)}(\mathbf{x})) \tag{4.7a}$$

and the matrix

$$\mathcal{V} = \begin{pmatrix} \mathcal{V}_{11}(\mathbf{x}) & \mathcal{V}_{12}(\mathbf{x}) \\ \mathcal{V}_{21}(\mathbf{x}) & \mathcal{V}_{22}(\mathbf{x}) \end{pmatrix} \tag{4.7b}$$

can be determined by two flows produced by two linearly independent pressure gradients

$$\overline{\boldsymbol{\nabla} p}^{(1)} = (1,0)^{\dagger}, \tag{4.7c}$$

$$\overline{\boldsymbol{\nabla} p}^{(2)} = (0,1)^{\dagger}. \tag{4.7d}$$

The first problem in the cell Q_0 yields the components $\bar{K}_{xx}$ and $\bar{K}_{xy}$ of the tensor $\bar{\mathbf{K}}$. Equation (3.17) implies

$$\mathcal{P}^{(1)}(\mathbf{a_m}+\mathbf{i}_1) - \mathcal{P}^{(1)}(\mathbf{a_m}) = \ell_1, \quad \mathcal{P}^{(1)}(\mathbf{a_m}+\mathbf{i}_2) - \mathcal{P}^{(1)}(\mathbf{a_m}) = 0. \tag{4.8a}$$

The condition (3.23) for the continuous medium implies

$$\mathcal{P}^{(1)}(\mathbf{x}+\mathbf{i}_1) - \mathcal{P}^{(1)}(\mathbf{x}) = \ell_1, \quad \mathcal{P}^{(1)}(\mathbf{x}+\mathbf{i}_2) - \mathcal{P}^{(1)}(\mathbf{x}) = 0. \tag{4.8b}$$

These pressure jumps (4.8a) and (4.8b) produce the flow with the velocity $(\mathcal{V}_{11}(\mathbf{x}),\mathcal{V}_{12}(\mathbf{x}))$, the pressure $\mathcal{P}^{(1)}(\mathbf{x})$, and the flow rate $\mathcal{J}_k^{(1)}$. Below instead of $(\mathcal{V}_{11}(\mathbf{x}),\mathcal{V}_{12}(\mathbf{x}))$, $\mathcal{P}^{(1)}(\mathbf{x})$, and $\mathcal{J}_k^{(1)}$ we write $\mathbf{v}(\mathbf{x})$, $p(\mathbf{x})$, and J_k, respectively, for shortness.

It follows from [6] that the component $\bar{v}_{cx}$ of the averaged seepage velocity along the x axis can be written as the integral along the two opposite vertical sides $L^{\pm}$ of the cell Q_0, (see Fig. 8)

$$\bar{v}_{cx} = \mathcal{S}^{-1}\left(\int_{L^+} - \int_{L^-}\right) x d\mathbf{s}\cdot\mathbf{v}_c = \ell_2^{-1}\int_{-\ell_2/2}^{\ell_2/2} v_x\left(\frac{\ell_1}{2},y\right)dy, \tag{4.9}$$

where $\mathbf{x}=(x,y)$.

Substitution of Eqs. (3.22) into Eq. (4.9) and the use of Eq. (4.6) yield for the xx component $\bar{K}_{xx}$ of the total macroscopic permeability tensor $\bar{\mathbf{K}}$,

$$\bar{K}_{xx} = \mathcal{S}^{-1}\left[\ell_1\int_{-\ell_2/2}^{\ell_2/2}\left(K_{xx}\frac{\partial p}{\partial x} + K_{xy}\frac{\partial p}{\partial y}\right)\bigg|_{x=\ell_1/2} dy + \sum_{k=1}^{M} X_k J_k\right], \tag{4.10}$$

where $K_{xx}(x,y)$ and $K_{xy}(x,y)$ are the components of the local permeability tensor $\mathbf{K}$ and $\mathbf{R}(k)=(X_k,Y_k)$. If the medium is homogeneous and isotropic, $\mathbf{K}=K\mathbf{I}$ and Eq. (4.10) becomes

$$\bar{K}_{xx} = \mathcal{S}^{-1}\left[K\ell_1\int_{-\ell_2/2}^{\ell_2/2}\frac{\partial p}{\partial x}\left(\frac{\ell_1}{2},y\right)dy + \sum_{k=1}^{M} X_k J_k\right]. \tag{4.11}$$

The macroscopic pressure gradient $\overline{\boldsymbol{\nabla}_p}^{(1)}$ also induces a flow along the y axis and a similar analysis yields $\bar{K}_{xy}$ by considering the flow through the lines M^+ and M^- (see Fig. 8)

$$\bar{K}_{xy} = \mathcal{S}^{-1}\left[K\ell_1\int_{-\ell_2/2}^{\ell_2/2}\frac{\partial p}{\partial y}\left(\frac{\ell_1}{2},y\right)dy + \sum_{k=1}^{M} Y_k J_k\right]. \tag{4.12}$$

The two other components $\bar{K}_{xy}$ and $\bar{K}_{yy}$ of the macroscopic permeability tensor can be obtained by considering the second problem when the pressure gradient is applied.

The first problem with given by Eq. (4.7c) is detailed in the rest of this paper and only the main lines are given for .

V. CONJUGATION PROBLEM

A. Statement of the problem

Consider now a conjugation problem which yields in a limit case the boundary value problems (3.28), (3.29), and (4.8b). This problem will prove useful to calculate the macroscopic permeability. Further, it is assumed that D_m are disks of sufficiently small radius r with centers at $\mathbf{a}_m$, i.e., $D_m=\{\mathbf{x}\in\mathbb{R}^2 : |\mathbf{x}-\mathbf{a}_m| < r\}$. More precisely,

$$|\mathbf{a}_k - \mathbf{a}_m| \geqslant r \quad \text{for all } m \neq k. \tag{5.1}$$

This assumption allows the application of the method of complex variables presented in [14,15], which yields constructive formulas for the local pressure and for the macroscopic permeability.

Let the perfectly permeable disks D_m of permeability K_1 be embedded in a host medium of permeability K. Then, the pressure in the disk D_m is described by a function $p_m(\mathbf{x})$, which is harmonic in D_m and continuously differentiable in its closure. The functions $p(\mathbf{x})$ and $p_m(\mathbf{x})$ satisfy the conjugation conditions

$$p^-(\mathbf{x}) = p^+(\mathbf{x}), \quad K\frac{\partial p^-}{\partial n}(\mathbf{x}) = K_1\frac{\partial p^+}{\partial n}(\mathbf{x}), \tag{5.2}$$

$$|\mathbf{x} - \mathbf{a}_m| = r, \quad m = 1,2, \dots ,N,$$

where $p^{\pm}$ denotes the limit values of the pressure in D_m and D, respectively; $\frac{\partial p^{\pm}}{\partial n}$ are analogously defined. The pressure $p(\mathbf{x})$ at D_m has the following asymptotic behavior:

$$p(\mathbf{x}) \sim q_m + \frac{j_m}{2\pi K_1}\ln|\mathbf{x} - \mathbf{a}_m|, \quad \text{as } \mathbf{x} \to \mathbf{a}_m, \quad m = 1,2, \dots ,N, \tag{5.3}$$

where q_m are constants. Here, the flow rate j_m is related to the pressure as follows:

$$j_m = -\sum_{k\in\Omega(m)} \alpha_k[\langle p_m\rangle - \langle p_{m'}(\mathbf{R}_{\mathbf{m}'})\rangle], \tag{5.4}$$

where $\mathbf{R}_{\mathbf{m}'}$ is given by Eq. (3.9); $\langle p_m\rangle$ denotes the mean pressure inside the disk D_m and $\langle p_{m'}(\mathbf{R}_{\mathbf{m}'})\rangle$ the mean pressure inside the disk $D_{m'}+\mathbf{R}_{\mathbf{m}'}$. In particular,

$$\langle p_{m'}(\mathbf{R}_{\mathbf{m}'})\rangle = \frac{1}{\pi r^2}\int_{D_{m'}} p_{m'}(\mathbf{x})d^2\mathbf{x} + \mathbf{R}_{\mathbf{m}'}\cdot\overline{\boldsymbol{\nabla}p}, \tag{5.5}$$

where $\overline{\boldsymbol{\nabla}p}$ is given by Eq. (4.7c).

B. Complex potentials

In application of the complex variable methods, the complex variable $z=x+iy \in \mathbb{C}$ is identified with the spatial variable $\mathbf{x}=(x,y) \in \mathbb{R}^2$. Following [14,15], complex periodic potentials based on Weierstrass's elliptic functions $\sigma(z)$ and $\zeta(z)$ can be introduced. The function $\ln\sigma(z)$ is analytic as well as $\ln z$ in the unit cell $\mathcal{Q}_0$ without a cut connecting the points $z=0$ and $z=\frac{\ell_1}{2}$. The behavior at zero is described by the following formula [14,15]:

$$\ln\sigma(z) = \ln z - \sum_{n=2}^{\infty}\frac{S_{2n}}{2n}z^{2n}, \tag{5.6}$$

where S_{2n} are the lattice sums calculated in [14,15]. The increments of $\ln\sigma(z)$ per cell are given by the two relations

$$\ln\sigma(z+\ell_1) - \ln\sigma(z) = \pi i + \ell_1 S_2\left(z + \frac{\ell_1}{2}\right), \tag{5.7a}$$

$$\ln\sigma(z+i\ell_2) - \ln\sigma(z) = \pi i - i\ell_2(2\pi - S_2)\left(z + \frac{i\ell_2}{2}\right). \tag{5.7b}$$

Introduce complex potentials $\varphi(z)$ and $\varphi_m(z)$ analytic in the disks D and D_m (see Fig. 8), respectively, in such a way that $\varphi(z)$ is doubly periodic and that the pressure is related to the complex potentials by

$$p(z) = \begin{cases} \mathrm{Re}[\varphi(z)+z], & z \in D, \\ \dfrac{2K}{K+K_1}\mathrm{Re}\left[\varphi_m(z) + \dfrac{K+K_1}{2K_1}\dfrac{j_m}{2\pi}\ln\sigma(z-a_m)\right], & z \in D_m, \end{cases} \tag{5.8}$$

where Re stands for the real part of a complex number. Here, the complex number a_m is identified with the center of the disk $\mathbf{a}_m$. Following [14,15], one can check that Eqs. (4.8b) and (5.3) are valid for such a choice of the complex potentials. The coefficient $2K/(K+K_1)$ in the second formula (5.8) is chosen for convenience in a first step; then, the macroscopic permeability is calculated in the limit $K_1 \to \infty$.

The first condition (5.2) becomes

$$\mathrm{Re}[\varphi(z)+z] = \frac{2K}{K+K_1}\mathrm{Re}\left[\varphi_m(z) + \frac{K+K_1}{2K_1}\frac{j_m}{2\pi}\ln\sigma(z-a_m)\right], \tag{5.9a}$$

$$|z - a_m| = r, \quad m = 1,2, \dots ,N.$$

The second condition (5.2) takes the form [13]

$$\mathrm{Im}[\varphi(z)+z] = \frac{2K_1}{K+K_1}\mathrm{Im}\left[\varphi_m(z) + \frac{K+K_1}{2K_1}\frac{j_m}{2\pi}\ln\sigma(z-a_m)\right],$$
$$|z - a_m| = r, \quad m = 1,2, \dots ,N. \tag{5.9b}$$

The two real equalities (5.9a) and (5.9b) can be combined as a complex relation

$$\varphi(z) + z = \varphi_m(z) + \frac{K+K_1}{2K_1}\frac{j_m}{2\pi}\ln\sigma(z-a_m) - \frac{K_1-K}{K_1+K}\left[\overline{\varphi_m(z)} + \frac{K+K_1}{2K_1}\frac{j_m}{2\pi}\ln\sigma(\overline{z-a_m})\right], \tag{5.10}$$

$$|z - a_m| = r, \quad m = 1,2, \dots ,N,$$

where the bar stands for the complex conjugation. Here, one uses the relation $\overline{\ln\sigma(z-a_m)} = \ln\sigma(\overline{z-a_m})$ on the circle $|z-a_m|=r$, which is based on Eq. (5.6) with the real coefficients S_{2n}.

Introduce Bergman's contrast parameter [20]

$$\rho = \frac{K_1 - K}{K_1 + K}. \tag{5.11}$$

Then, $\frac{K_1+K}{2K_1} = \frac{1}{1+\rho}$. Using the relation $\overline{z-a_m} = \frac{r^2}{z-a_m}$ on the circle $|z-a_m| = r$, Eq. (5.10) can be rewritten in the form of an $\mathbb{R}$-linear problem [13]

$$\varphi(z) = \varphi_m(z) - \rho\overline{\varphi_m(z)} + f_m(z), \tag{5.12}$$

$$|z - a_m| = r, \quad m = 1,2, \ldots ,N,$$

where

$$f_m(z) = -z + \frac{j_m}{2\pi}\ln(z-a_m) + \frac{j_m}{2\pi}\left[-\frac{2\rho}{1+\rho}\ln r + F(z-a_m) - \rho F\left(\frac{r^2}{z-a_m}\right)\right]. \tag{5.13}$$

The function $F(z)$ is introduced via Eq. (5.6) as follows:

$$F(z) = \ln\frac{\sigma(z)}{z} = -\sum_{n=2}^{\infty}\frac{S_{2n}}{2n}z^{2n}. \tag{5.14}$$

$F(z)$ is analytic in $\mathcal{Q}_0$ since $\sigma(z)$ has a unique zero at $z=0$ in $\mathcal{Q}_0$.

Instead of Eq. (5.12), it is convenient to study the $\mathbb{R}$-linear problem for the derivatives $\varphi'(z) = \psi(z)$, $\varphi'_m(z) = \psi_m(z)$, which becomes [13]

$$\psi(z) = \psi_m(z) + \rho\left(\frac{r^2}{z-a_m}\right)^2\overline{\psi_m(z)} + f'_m(z), \tag{5.15}$$

$$|z - a_m| = r, \quad m = 1,2, \ldots ,N,$$

where

$$f'_m(z) = -1 + \frac{j_m}{2\pi}\left[\frac{1}{z-a_m} + f(z-a_m) + \rho\left(\frac{r^2}{z-a_m}\right)^2 f\left(\frac{r^2}{z-a_m}\right)\right]. \tag{5.16}$$

The function $f(z)$ is defined as

$$f(z) = F'(z) = \zeta(z) - \frac{1}{z}, \tag{5.17}$$

where $\zeta(z)$ is the Weierstrass ζ function. $f(z)$ is analytic in $\mathcal{Q}_0$ and represented by the series

$$f(z) = -\sum_{n=2}^{\infty} S_{2n}z^{2n-1}. \tag{5.18}$$

C. Macroscopic continuous permeability

The component $\bar{K}_{xx}$ of the macroscopic permeability tensor (4.6) can be calculated by using Eqs. (4.1), (4.2), and (4.11),

$$\bar{K}_{xx} = \mathcal{S}^{-1}\left(K\int_D \frac{\partial p}{\partial x}d^2\mathbf{x} + K_1\sum_{m=1}^{N}\int_{D_m}\frac{\partial p}{\partial x}d^2\mathbf{x} - \sum_{m=1}^{N}x_m j_m + \sum_{k=1}^{M}X_k J_k\right). \tag{5.19}$$

Green's formula implies

$$\int_D \frac{\partial p}{\partial x}d^2\mathbf{x} = \int_{\partial\mathcal{Q}_0} p\,dy - \sum_{m=1}^{N}\int_{\partial D_m} p^- dy. \tag{5.20}$$

Because of Eq. (4.8b),

$$\int_{\partial\mathcal{Q}_0} p\,dy = \int_{-\ell_2/2}^{\ell_2/2}[p(x+\ell_1,y) - p(x,y)]dy = \mathcal{S}. \tag{5.21}$$

Substitution of Eqs. (5.20) and (5.21) into Eq. (5.19) and the use of the first relation (5.2) yield

$$\bar{K}_{xx} = K + (K_1 - K)\mathcal{S}^{-1}\sum_{m=1}^{N}\int_{\partial D_m} p^+ dy + \frac{1}{\mathcal{S}}\left(\sum_{k=1}^{M}X_k J_k - \sum_{m=1}^{N}x_m j_m\right). \tag{5.22}$$

Introduction of the complex potentials (5.8) into (5.22) yields

$$\frac{\bar{K}_{xx}}{K} = 1 + \frac{2\rho}{\mathcal{S}}\sum_{m=1}^{N}\int_{\partial D_m}\text{Re}\,\varphi_m(z)dy + \frac{K_1-1}{\mathcal{S}K_1}\sum_{m=1}^{N}\frac{j_m}{2\pi}\int_{\partial D_m}\ln|\sigma(z-a_m)|dy + \frac{1}{\mathcal{S}K}\left(\sum_{k=1}^{M}X_k J_k - \sum_{m=1}^{N}x_m j_m\right). \tag{5.23}$$

The first integral in Eq. (5.23) is calculated by the mean value theorem of the harmonic function theory [21]

$$\int_{\partial D_m}\text{Re}\,\varphi_m(z)dy = \pi r^2\,\text{Re}\,\psi_m(a_m). \tag{5.24}$$

The second integral is equal to zero since according to Eq. (5.6),

$$\int_{|t|=r}\ln|\sigma(t)|dy = \int_0^{2\pi}\left(\ln r - \sum_{n=2}^{\infty}\frac{S_{2n}}{2n}r^{2n}\cos 2n\theta\right)r\cos\theta d\theta = 0, \tag{5.25}$$

where $t = re^{i\theta}$. Therefore, Eq. (5.23) becomes

$$\frac{\bar{K}_{xx}}{K} = 1 + 2\rho\nu\frac{1}{N}\sum_{m=1}^{N}\text{Re}\,\psi_m(a_m) + \frac{1}{\mathcal{S}K}\left(\sum_{k=1}^{M}X_k J_k - \sum_{m=1}^{N}x_m j_m\right), \tag{5.26}$$

where $\nu = \mathcal{S}^{-1}N\pi r^2$ is the relative area of inclusions per cell.

Formula (5.26) is convenient since it is sufficient to take $\rho=1$ [see Eq. (5.11)] to obtain the limit $K_1\to\infty$. According to [16], one can deduce the following formula:

$$\frac{\bar{K}_{xx}-i\bar{K}_{xy}}{K}=1+\frac{2\nu}{N}\sum_{m=1}^{N}\psi(a_m)+\frac{1}{\mathcal{S}K}\left(\sum_{k=1}^{M}Z_kJ_k-\sum_{m=1}^{N}\overline{a_m}j_m\right), \tag{5.27}$$

where $Z_k=X_k-iY_k$ is the conjugated value to the complex coordinate of the vector $\mathbf{R}(k)$, and $\overline{a_m}$ is conjugated to a_m. The two other components $\bar{K}_{xy}$ and $\bar{K}_{yy}$ can be obtained by the second problem when the macroscopic pressure gradient is given by Eq. (5.7b) They can also be calculated by a rotation of the cell by 90° and a formal application of Eq. (5.27).

VI. SOLUTION

A. Solution to the continuous problem in the zeroth approximation

As noted at the end of Sec. III B, the solution of the network problem requires the continuous problem to be solved. Therefore, let us solve it in the zeroth approximation in r. As will be seen later, this approximation is not generally sufficient, but it can be applied to construct a nontrivial first approximation for the macroscopic continuous permeability.

Consider the continuous problem stated in Sec. III C when the domains D_m are contracted down to the points a_m. Then, the problem is reduced to the determination of the function $p(z)$ harmonic in $\mathcal{Q}_0$ except at the points a_m where

$$p(z)\sim q_m+\frac{j_m}{2\pi}\ln|z-a_m|,\quad \text{as } z\to a_m. \tag{6.1}$$

Therefore, one can look for $p(z)$ in the form

$$p(z)=\sum_{m=1}^{N}\frac{j_m}{2\pi}\ln|\sigma(z-a_m)|+\mathrm{Re}[Az]+p_0, \tag{6.2}$$

with an undetermined complex constant A and a real constant p_0. The constant p_0 does not impact on j_m because of Eqs. (3.18) and (3.19). Equations (5.7) and (3.35) yield the increments of $p(z)$ along the x axis,

$$p(z+\ell_1)-p(z)=\sum_{m=1}^{N}\frac{j_m}{2\pi}\mathrm{Re}\left[\pi i+\ell_1S_2\left(z-a_m+\frac{\ell_1}{2}\right)\right]+\ell_1\,\mathrm{Re}\,A=\ell_1\left[-\frac{S_2}{2\pi}\sum_{m=1}^{N}j_mx_m+\mathrm{Re}\,A\right]. \tag{6.3}$$

Along similar lines,

$$p(z+i\ell_2)-p(z)=-\ell_2\left[\left(1-\frac{S_2}{2\pi}\right)\sum_{m=1}^{N}j_my_m+\mathrm{Im}\,A\right]. \tag{6.4}$$

The constant A is derived from the conditions (4.8b),

$$A=1+\frac{S_2}{2\pi}\sum_{m=1}^{N}j_ma_m-i\sum_{m=1}^{N}j_my_m. \tag{6.5}$$

Then, Eqs. (5.2) and (5.5) express the function p through j_m up to an additive constant p_0.

$p(z)$ can be estimated on the circle ∂D_m up to $O(r)$. Introduce the local polar coordinates $z=a_m+re^{i\theta}$ near a fixed circle ∂D_m. Then,

$$p(a_m+re^{i\theta})=\frac{j_m}{2\pi}\ln|\sigma(re^{i\theta})|+\sum_{k\neq m}\frac{j_k}{2\pi}\ln|\sigma(a_m-a_k+re^{i\theta})|+\mathrm{Re}[A(a_m+re^{i\theta})]+p_0. \tag{6.6}$$

When the terms of order $O(r)$ are neglected, Eq. (6.6) implies

$$p_m=\frac{j_m}{2\pi}\ln r+\sum_{k\neq m}\frac{j_k}{2\pi}\ln|\sigma(a_m-a_k)|+\mathrm{Re}[Aa_m]+p_0,\quad m=1,2,\ldots,N, \tag{6.7}$$

where A is linearly related to j_m $(m=1,\ldots,N)$ by Eq. (6.6).

B. Solution in the network

In the present section, the method of solution to the network problem stated in Sec. III B is modified according to [5,6]. To combine Eqs. (3.17)–(3.21) into more compact formulas, the flow rate vector $\mathbf{J}=(J_1,J_2,\ldots,J_m)^\dagger$ is introduced where $\mathbf{X}^\dagger$ stands for the transposed vector of $\mathbf{X}$. The components of $\mathbf{J}$ represent the algebraic flow rate with respect to the orientation of Γ [see Eq. (3.18)] on the edge e_k.

The components of the pressure difference vector $\mathbf{P}$ are equal to the pressure differences between the vertices such that [see Eq. (3.17)]

$$P_k=p_m-p_{m'}(\mathbf{a}_{m'}+\mathbf{R}_{\mathbf{m}'}),\quad e_k=\{\mathbf{a}_m,\mathbf{a}_{m'}\},\quad \mathbf{a}_m\in\mathcal{Q}_0. \tag{6.8}$$

Here, the short designation p_m instead of $p_m(\mathbf{a}_m)$ is used in accordance with Eq. (6.7). The $M\times M$ diagonal conductance matrix Λ is defined as follows:

$$\Lambda_{kk}=\begin{cases}0 & \text{if } e_k \text{ joins homologous vertices}\\ \alpha_k^{-1} & \text{otherwise.}\end{cases} \tag{6.9}$$

The network is energized by a generator acting between homologous vertices of the periodic graph in the x direction. Let $e_k=(\mathbf{a}_m,\mathbf{a}_{m'})$ be an edge joining the homologous vertices $\mathbf{a}_m\in\mathcal{Q}_0$ and $\mathbf{a}_{m'}\in\mathcal{Q}_0\pm\mathbf{i}_1$. Following [5,6], a pressure generator is introduced whose component on e_k is given by

$$G_k=\begin{cases}1 & \text{if } e_k \text{ crosses } L^+\\ -1 & \text{if } e_k \text{ crosses } L^-\\ 0 & \text{if } e_k \text{ does not cross } L^\pm,\end{cases} \tag{6.10}$$

where L^+ and L^- are the right and the left vertical sides, respectively, of the rectangle $\mathcal{Q}_0$ (see Fig. 8). Here, at least one of the vertices of e_k belongs to the zeroth cell $\mathcal{Q}_0$. The M relations in Eq. (4.10) for the pressure generator can be expressed in the vector form

$$\mathbf{G} = \mathcal{R}\overline{\boldsymbol{\nabla} p}^{(1)}, \tag{6.11}$$

where $\mathbf{G}=(G_1,G_2,\ldots,G_M)^\dagger$; the components of the $2\times M$ matrix $\mathcal{R}$ are equal to -1, 0, $+1$ in accordance with Eq. (6.10).

The basic equations governing the network flow can be expressed in matricial form. Equation (3.18) becomes

$$\mathbf{P} = \Lambda \cdot \mathbf{J} + \mathbf{G}. \tag{6.12}$$

The conservation equation (3.19) of the fluid at each vertex can be written in a simple form by using the incidence matrix

$$\mathbf{D} \cdot \mathbf{J} = \mathbf{j}, \tag{6.13}$$

where $\mathbf{j}=(j_1,j_2,\ldots,j_N)^\dagger$.

Kirchhoff's potential law states that along every cycle of the graph, the pressure difference is equal to zero. Therefore,

$$\xi_Q \cdot \mathbf{P} = 0, \tag{6.14}$$

where ξ_Q runs over the cycle vectors of Γ. The latter equation can be written in the form (see details in [5,6])

$$\mathbf{C}^\dagger \cdot \mathbf{P} = \mathbf{0}, \tag{6.15}$$

where the matrix $\mathbf{C}$ is introduced above in Eq. (3.14).

Finally, Eq. (6.7) can be transformed as follows. Choose a spanning tree T in the graph Γ. Introduce the vectors $\mathbf{P}_T$ and $\mathbf{P}_S$ of dimensions $N-1$ and $M-N+1$ in such a way that

$$\mathbf{P} = \begin{pmatrix} \mathbf{P}_T \\ \mathbf{P}_S \end{pmatrix}. \tag{6.16}$$

The cut vector of the flow rates $\mathbf{j}^*=(j_1,j_2,\ldots,j_{N-1})^\dagger$ is used below. It is worth noting that if $\mathbf{j}^*$ is known, j_N is easily found by Eq. (3.35). Using Eqs. (6.7) (if the vertices $\mathbf{a}_m,\mathbf{a}_{m'}$ are not homologous) and (3.17) (if they are), the difference $p_m-p_{m'}$ is calculated when the edge $(\mathbf{a}_m,\mathbf{a}_{m'})$ belongs to the tree T. Then, a linear dependence is obtained,

$$\mathbf{P}_T = \mathbf{A} \cdot \mathbf{j}^* - \mathbf{a}, \tag{6.17}$$

with a square matrix $\mathbf{A}$ of dimension $(N-1)\times(N-1)$ and the vector $\mathbf{a}$ whose coordinates are $x_{m'}-x_m$. Here, Eq. (3.35) is used to eliminate j_N. In order to demonstrate that the matrix $\mathbf{A}$ is invertible, it is sufficient to show that the homogeneous system

$$\mathbf{P}_T = \mathbf{A} \cdot \mathbf{j}^* \tag{6.18}$$

has only the trivial solution $\mathbf{j}^*=\mathbf{0}$ if $\mathbf{P}_T=\mathbf{0}$. The latter follows from the physical arguments since the system (6.18) corresponds to the absence of external forces. Then, $\mathbf{P}_T=\mathbf{0}$ yields that the pressure is constant at each vertex of the network. This implies that all j_m have to be equal to zero.

One can propose the following method to calculate $\mathbf{A}^{-1}$. First, consider Eq. (6.17) as a system of linear algebraic equations with respect to $j_m-j_{m'}$ where $(\mathbf{a}_m,\mathbf{a}_{m'})$ belongs to the tree T. This system has a dominated diagonal matrix with the dominated terms $\frac{1}{2\pi}\ln r$ at the diagonal elements because of Eq. (5.1). Then, the matrix corresponding to the latter system is invertible and $j_m-j_{m'}$ can be written as a linear combination of the $N-1$ components of $\mathbf{P}_T$. Further, a simple algorithm associated to the tree T can be applied to equations $j_m-j_{m'}=b_k$ $(k=1,2,\ldots,N-1)$. This algorithm is based on the choice of one end point of the tree T with a fixed flow rate, say j_s, and successive determination of the other flow rates via j_s by linear operations. At the last step, formula (3.35) is used to find j_s. Thus, we obtain

$$\mathbf{j}^* = \mathbf{A}^{-1} \cdot (\mathbf{P}_T + \mathbf{a}). \tag{6.19}$$

Hence, Eqs. (6.12), (6.13), (6.15), and (6.19) are equivalent to M, $N-1$, $M-N+1$, and $N-1$ scalar equations. Here, one scalar equation is excluded from the set of equations (6.13) since the matrix $\mathbf{D}$ has the following property [5,6]. When all the scalar equations of Eq. (6.13) are added, the result in the left-hand side gives zero for any vector $\mathbf{J}$. Therefore, Eq. (3.35) can be considered as a necessary condition of solvability of Eq. (6.13).

The systems (6.12), (6.13), (6.15), and (6.19) can be solved by the following method. Similar to Eq. (6.16), $\mathbf{J}$ can be written as

$$\mathbf{J} = \begin{pmatrix} \mathbf{J}_T \\ \mathbf{j}_S \end{pmatrix}. \tag{6.20}$$

Using the decomposition (3.15), Eq. (6.13) is expressed as

$$\mathbf{D}_T \cdot \mathbf{J}_T + \mathbf{D}_S \cdot \mathbf{J}_S = \mathbf{j}^*. \tag{6.21}$$

Observe that the last row of $\mathbf{D}$ is not used. Substitute $\mathbf{j}^*$ from Eq. (6.19) into Eq. (6.21),

$$\mathbf{D}_T \cdot \mathbf{J}_T + \mathbf{D}_S \cdot \mathbf{J}_S = \mathbf{A}^{-1} \cdot (\mathbf{P}_T + \mathbf{a}). \tag{6.22}$$

Application of Eq. (3.16) to Eq. (6.22) yields

$$\mathbf{J}_T = \mathbf{C}_T \cdot \mathbf{J}_S + \mathbf{D}_T^{-1} \cdot \mathbf{A}^{-1} \cdot (\mathbf{P}_T + \mathbf{a}). \tag{6.23}$$

Equivalently, by employing the decomposition (3.15) of $\mathbf{C}$,

$$\mathbf{J} = \mathbf{C} \cdot \mathbf{J}_S + \begin{pmatrix} \mathbf{D}_T^{-1} \cdot \mathbf{A}^{-1} \cdot (\mathbf{P}_T + \mathbf{a}) \\ \mathbf{0}_{M-N+1} \end{pmatrix}, \tag{6.24}$$

where $\mathbf{0}_{M-N+1}$ denotes the zero matrix of dimension $M-N+1$. Introduction of the latter expression into Eq. (6.12) yields

$$\mathbf{P} = \Lambda \cdot \left[\mathbf{C} \cdot \mathbf{J}_S + \begin{pmatrix} \mathbf{D}_T^{-1} \cdot \mathbf{A}^{-1} \cdot (\mathbf{P}_T + \mathbf{a}) \\ \mathbf{0}_{M-N+1} \end{pmatrix} \right] + \mathbf{G}. \tag{6.25}$$

Two equations can be deduced from Eq. (6.25). First, take the component of $\mathbf{P}_T$ from Eq. (6.25). This corresponds to the multiplication by a diagonal matrix $\mathbf{E}$ with $E_{kk}=1$ if $k\in T$ and $E_{kk}=0$ otherwise. Then, Eq. (6.25) implies that

$$\mathbf{P}_T = \mathbf{E} \cdot \Lambda \cdot \left[\mathbf{C} \cdot \mathbf{J}_S + \begin{pmatrix} \mathbf{D}_T^{-1} \cdot \mathbf{A}^{-1} \cdot (\mathbf{P}_T + \mathbf{a}) \\ \mathbf{0}_{M-N+1} \end{pmatrix} \right] + \mathbf{E} \cdot \mathbf{G}. \tag{6.26}$$

The second equation is obtained by multiplication of Eq. (6.25) by $\mathbf{C}^\dagger$ to eliminate $\mathbf{P}$ [see Eq. (6.15)]. Hence,

$$\mathbf{C}^{\dagger}\cdot\mathbf{\Lambda}\cdot\mathbf{C}\cdot\mathbf{J}_S+\mathbf{C}^{\dagger}\cdot\begin{pmatrix}\mathbf{D}_T^{-1}\cdot\mathbf{A}^{-1}\cdot(\mathbf{P}_T+\mathbf{a})\\ \mathbf{0}_{M-N+1}\end{pmatrix}+\mathbf{C}^{\dagger}\cdot\mathbf{G}=\mathbf{0}. \tag{6.27}$$

Since the matrix $\mathbf{C}^{\dagger}\cdot\Lambda\cdot\mathbf{C}$ is invertible [5,6], it is possible to express

$$\mathbf{J}_S=-(\mathbf{C}^{\dagger}\cdot\Lambda\cdot\mathbf{C})^{-1}\cdot\mathbf{C}^{\dagger}\cdot\begin{pmatrix}\mathbf{D}_T^{-1}\cdot\mathbf{A}^{-1}\cdot(\mathbf{P}_T+\mathbf{a})\\ \mathbf{0}_{M-N+1}\end{pmatrix}-(\mathbf{C}^{\dagger}\cdot\Lambda\cdot\mathbf{C})^{-1}\cdot\mathbf{C}^{\dagger}\cdot\mathbf{G}. \tag{6.28}$$

Substitution of Eq. (6.28) into Eq. (6.26) yields

$$\mathbf{P}_T=\mathbf{E}\cdot\mathbf{\Lambda}\cdot[\mathbf{I}_M-\mathbf{C}\cdot(\mathbf{C}^{\dagger}\cdot\Lambda\cdot\mathbf{C})^{-1}\cdot\mathbf{C}^{\dagger}]\cdot\begin{pmatrix}\mathbf{D}_T^{-1}\cdot\mathbf{A}^{-1}\cdot(\mathbf{P}_T+\mathbf{a})\\ \mathbf{0}_{M-N+1}\end{pmatrix}+\mathbf{E}\cdot[\mathbf{I}_M-\Lambda\cdot\mathbf{C}\cdot(\mathbf{C}^{\dagger}\cdot\Lambda\cdot\mathbf{C})^{-1}\cdot\mathbf{C}^{\dagger}]\cdot\mathbf{G}. \tag{6.29}$$

One can consider Eq. (6.29) as $N-1$ scalar equations with respect to the $N-1$ components of the vector $\mathbf{P}_T$. The right-hand side of this system is proportional to $\overline{\boldsymbol{\nabla} p}$ via $\mathbf{G}$ and to $\mathbf{a}$.

C. Solution in the continuum

A constructive solution to the $\mathbb{R}$-linear problem (5.15) in a class of doubly periodic functions is possible with the methods presented and developed in [13]. Simple approximate formulas for ψ_m up to $O(r^2)$ are used to estimate $\bar{K}_{xx}$ up to $O(\nu^2)$. Consider the problem (5.15) for small r relative to the distances between the centers. Then, Eq. (5.15) up to $O(r^2)$ yields

$$\psi^{(0)}(z)=\psi_m^{(0)}(z)-1+\frac{j_m}{2\pi}\zeta(z-a_m), \tag{6.30}$$

$$|z-a_m|=r,\quad m=1,2,\ldots,N.$$

The relation (6.30) can be considered as a $\mathbb{C}$-linear problem [13] in a class of doubly periodic functions. One can check that its solution has the form

$$\psi^{(0)}(z)=\sum_{k=1}^{N}\frac{j_k}{2\pi}\zeta(z-a_k),\quad z\in D,$$

$$\psi_m^{(0)}(z)=1+\sum_{k\neq m}\frac{j_k}{2\pi}\zeta(z-a_k), \tag{6.31}$$

$$|z-a_m|\leq r,\quad m=1,2,\ldots,N.$$

Substitute the zeroth approximation for $\psi_m(a_m)$ into Eq. (5.27),

$$\frac{\bar{K}_{xx}-i\bar{K}_{xy}}{K}\approx 1+2\nu\left[1+\frac{1}{N}\sum_{k=1}^{N}\sum_{k\neq m}\frac{j_k}{2\pi}\zeta(a_m-a_k)\right]+\frac{1}{\mathcal{S}K}\left(\sum_{k=1}^{M}Z_kJ_k-\sum_{m=1}^{N}\overline{a_m}j_m\right). \tag{6.32}$$

Use of Eqs. (4.4) and (4.12) yields the components of the total permeability tensor

$$\frac{\bar{K}_{xx}-i\bar{K}_{xy}}{K}\approx\frac{1+\nu\left[1+\frac{1}{N}\sum_{k=1}^{N}\sum_{k\neq m}\frac{j_k}{2\pi}\zeta(a_m-a_k)\right]}{1-\nu\left[1+\frac{1}{N}\sum_{k=1}^{N}\sum_{k\neq m}\frac{j_k}{2\pi}\zeta(a_m-a_k)\right]}+\frac{1}{\mathcal{S}K}\left(\sum_{k=1}^{M}Z_kJ_k-\sum_{m=1}^{N}\overline{a_m}j_m\right), \tag{6.33}$$

where J_k is the flow rate given by Eq. (3.18). This formula for $J_k=0$ ($j_m=0$) becomes the classical Clausius-Mossotti approximation [17].

D. Discussion

Equation (6.33) provides the total permeability of a two-dimensional spatially periodic porous medium with punctual resurgences.

The method can now be summarized and its order of approximation justified. In Sec. VI A, the continuous problem in the zeroth approximation yields formula (6.7), which relates the pressure p_m with fixed m and the flow rates j_k ($k=1,2,\ldots,N$) near a_m. This formula contains $\ln r$ and constant on r terms; hence, it is deduced up to $O(r)$. The discrete algorithm from [5,6] in Sec. VI B is used to solve the network problem added by the relation (6.7) and to determine j_m. Therefore, the network problem is solved up to $O(r)$. The flow rates j_m are found with the accuracy $O(r\ln^{-1}r)$ since the inverse of the diagonal dominated matrix in Eq. (6.7) is proportional to $\ln^{-1}r$. It follows from Eqs. (6.24), (6.19), and (6.28) that J_k are found also within $O(r\ln^{-1}r)$.

In Sec. VI C, we return to the continuous phase and use the known parameters j_m to completely solve the continuous problem with the accuracy $O(r)$. As a result, formula (6.33) for the total macroscopic permeability is derived and is valid with the accuracy $O(r\ln^{-1}r)$.

It is interesting to note that formula (6.33) contains the locations of inclusions a_m in contrast with the classical Clausius-Mossotti approximation. This means that the presence of the network essentially changes the macroscopic permeability even in the "dilute" case.

VII. EXAMPLES

A. Square lattice

Consider the unit square lattice of the disks ($\ell_1=\ell_2=1$) and the associated square network as shown in Fig. 9.

In this case $N=1$ and $j_1=0$ because of Eq. (3.35). Then, flow occurs separately through the network and the continuous phase. Equation (5.27) implies

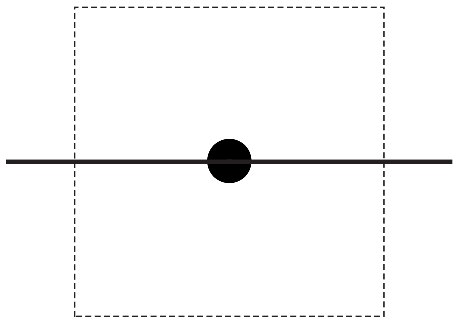

FIG. 9. The unit cell of the square lattice.

$$\frac{\bar{K}_{xx}}{K} \approx \frac{1+\nu}{1-\nu} + \frac{\alpha}{K}, \quad \bar{K}_{xy} = 0, \quad \frac{\bar{K}_{yy}}{K} \approx \frac{1+\nu}{1-\nu}. \tag{7.1}$$

The formulas for $\bar{K}_{xx}$ and $\bar{K}_{yy}$ can be given in an exact form by using the exact formula for $\bar{K}_{yy}$ [16].

B. Square lattice with connections

Consider the unit square lattice of the disks and the associated square network as shown in Fig. 10. In this example, $a_1=\frac{1}{4}$, $a_2=-\frac{1}{4}$, $j_1=-j_2$; one can take $p_1=-p_2$ up to an additive constant. Then, Eq. (6.7) becomes

$$p_1 = \frac{j_1}{2\pi}\left[\ln r - \ln\left|\sigma\left(\frac{1}{2}\right)\right| + \frac{\pi}{2}\right] + \frac{1}{4}$$
$$= \frac{j_1}{2\pi}(\ln r + 0.826\,25) + \frac{1}{4}. \tag{7.2}$$

Equation (3.18) implies

$$J_1 = \alpha(p_2 - p_1) = -2\alpha p_1 = -\frac{\alpha j_1}{2\pi}\left[\ln\frac{r}{\left|\sigma\left(\frac{1}{2}\right)\right|} + \frac{\pi}{2}\right] - \frac{\alpha}{2}. \tag{7.3}$$

Since $j_1=J_1$,

$$j_1 = -\frac{\alpha j_1}{2\pi}(\ln r + 0.826\,25) - \frac{\alpha}{2}. \tag{7.4}$$

One can find

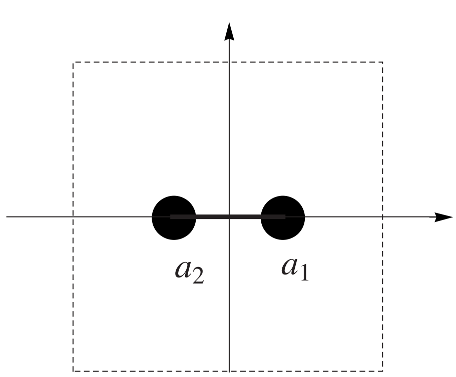

FIG. 10. The unit cell with two disks.

$$j_1 = -\frac{\alpha}{2\left[1 + \frac{\alpha}{\pi}(\ln r + 0.826\,25)\right]}. \tag{7.5}$$

Then, because of Eqs. (4.4) and (6.33), and $K_n=\mathbf{0}$ we get

$$\bar{K}_{xx} \approx \frac{1+\nu\left[1+\frac{j_1}{2\pi}\zeta\left(\frac{1}{2}\right)\right]}{1-\nu\left[1+\frac{j_1}{2\pi}\zeta\left(\frac{1}{2}\right)\right]} + \frac{j_1}{K}, \quad \bar{\mathbf{K}}_{xy} = 0, \tag{7.6a}$$

where j_1 has the form (7.5), $\zeta\left(\frac{1}{2}\right)=1.5708$. One can see that

$$\bar{K}_{yy} \approx \frac{1+\nu}{1-\nu}. \tag{7.6b}$$

VIII. CONCLUSION

The present investigation opens up a whole class of new problems which can be extended in many different ways. Because of the nonlocal character of the equations, it can be expected that new mathematical techniques will be necessary to address, for instance, extended resurgences which are partially governed by Eq. (3.31).

The main physical extensions can be provisorily listed as follows. The first one consists of three-dimensional situations which are much more interesting from a practical point of view. As already said, the formalism which has been introduced is general and it is only the resolution of the equations which is much more difficult even in the "dilute" approximation for punctual resurgences. The case of three-dimensional extended resurgences is particularly challenging since unexpected effects such as the ones displayed in Fig. 4 will probably arise.

The second extension consists of time-dependent problems which are also very important; compressibility effects should be taken into account as in the well tests which are routinely performed in the oil industry. In such cases, the capillaries may also work as capacities able to store fluid. Very different behaviors are likely to occur.

APPENDIX: DETERMINATION OF THE MACROSCOPIC PERMEABILITY

The derivation is made for a three-dimensional medium, but it can be restricted without any difficulty to two dimensions. Since the velocity field $\mathbf{v}$ is divergence-free, it can be written as

$$\mathbf{v} = \nabla \cdot (\mathbf{v}\mathbf{x}). \tag{A1}$$

The total seepage velocity $\bar{\mathbf{v}}$ can be expressed as

$$\bar{\mathbf{v}} = \frac{1}{\tau}\left[\int_{\tau_m} \mathbf{v}\, d^3\mathbf{x} + \int_{V_{cb}} \mathbf{v}\, d^3\mathbf{x}\right], \tag{A2a}$$

where the total volume τ is the sum of the volumes of the continuous porous medium τ_m and of the capillary network V_{cb} in the basic graph. In most cases, V_{cb} is negligible with respect to τ_m,

$$\tau = \tau_m + V_{cb} \approx \tau_m. \tag{A2b}$$

The first integral can be transformed with the help of Eq. (A1) and of the divergence theorem

$$\int_{\tau_m} \mathbf{v} d^3\mathbf{x} = \int_{\partial\tau_m} \mathbf{x} d\mathbf{s} \cdot \mathbf{v} + \sum_{m \in \tau_m} \int_{S_{mc}} \mathbf{x} d\mathbf{s} \cdot \mathbf{v}, \tag{A3}$$

where $\partial\tau_m$ is the external surface of the unit cell and S_{mc} is the interface between the capillaries and the continuous medium. $d\mathbf{s}$ is oriented outwards of τ_m.

The second integral can be written as a sum over the basic graph of integrals over the volume of each capillary

$$\mathbf{I}_{cb} = \int_{V_{cb}} \mathbf{v} d^3\mathbf{x} = \sum_{k=1}^{M} \int_{v_c(k)} \mathbf{v} d^3\mathbf{x}, \tag{A4}$$

where M is the number of edges in the basic graph. The same technique as before can be applied. Since the fluid velocity vanishes at the surface of the capillaries, one obtains

$$\mathbf{I}_{cb} = \sum_{k=1}^{M} \left[\int_{S^-(k)} \mathbf{R}_k^- d\boldsymbol{\sigma}^- \cdot \mathbf{v} + \int_{S^+(k)} \mathbf{R}_k^+ d\boldsymbol{\sigma}^+ \cdot \mathbf{v} \right], \tag{A5}$$

where $d\boldsymbol{\sigma}^\pm$ are surface elements oriented from the interior to the exterior of the capillaries. The position vector $\mathbf{R}$ can be decomposed into its global part $\mathbf{R}_\mathbf{I}$ when the vertex belongs to the cell referred to by $\mathbf{I}$ and its local part $\mathbf{r}$,

$$\mathbf{R}_k^\pm = \mathbf{R}_{\mathbf{I}^\pm} + \mathbf{r}. \tag{A6}$$

Therefore,

$$\begin{aligned}\mathbf{I}_{cb} &= \sum_{k=1}^{M} \left[\int_{S^-(k)} (\mathbf{R}_{\mathbf{I}^-} + \mathbf{r}) d\boldsymbol{\sigma}^- \cdot \mathbf{v} + \int_{S^+(k)} (\mathbf{R}_{\mathbf{I}^+} + \mathbf{r}) d\boldsymbol{\sigma}^+ \cdot \mathbf{v} \right] \\ &= \sum_{k=1}^{M} \mathbf{R}(k) J_k + \sum_{k=1}^{M} \left[\int_{S^-(k)} \mathbf{r} d\boldsymbol{\sigma}^- \cdot \mathbf{v} + \int_{S^+(k)} \mathbf{r} d\boldsymbol{\sigma}^+ \cdot \mathbf{v} \right],\end{aligned} \tag{A7}$$

where $\mathbf{R}(k) J_k = \mathbf{R}_{\mathbf{I}^+} - \mathbf{R}_{\mathbf{I}^-}$.

Let us now examine the second sum in Eq. (A7). Consider a vertex internal to the network, i.e., without any resurgence to communicate with the porous medium. The sum of all the flow rates which come from the incident edges is equal to the sum of all the flow rates which come from the outgoing edges; the sum of the corresponding terms is equal to 0. Next, consider vertices with resurgence and compare the corresponding terms to the second term in the right-hand side of Eq. (A3). It is an easy matter to realize that they are equal and opposite since $d\mathbf{s} = -d\boldsymbol{\sigma}$.

Therefore, the total seepage velocity $\overline{\mathbf{v}}$ is equal to

$$\overline{\mathbf{v}} = \frac{1}{\tau} \left[\int_{\partial\tau_m} \mathbf{x} d\mathbf{s} \cdot \mathbf{v} + \sum_{k=1}^{M} \mathbf{R}(k) J_k \right]. \tag{A8}$$

[1] G. I. Barenblatt, I. P. Zheltov, and I. N. Kochina, Sov. Appl. Math. Mech., (P. M. M.) **24**, 852 (1960).

[2] I. I. Bogdanov, V. V. Mourzenko, J.-F. Thovert, and P. M. Adler, Water Resour. Res. **39**, 10.1029/2001WR000756 (2003).

[3] M. Barthélémy and Luis A. Nunes Amaral, Phys. Rev. Lett. **82**, 3180 (1999).

[4] D. Gibert, F. Nicollin, B. Kergosien, P. Bossart, C. Nussbaum, A. Grislin-Mouëzy, F. Conil, and Nasser Hoteit, Appl. Clay Sci. **33**, 21 (2006).

[5] P. M. Adler and H. Brenner, PCH, PhysicoChem. Hydrodyn. **5**, 245 (1984).

[6] P. M. Adler, *Porous Media. Geometry and Transport* (Butterworth-Heinemann, Stoneham, Ma, 1992).

[7] L. Berlyand and A. Kolpakov, *Introduction into Network Approximation for Contrast Boundary-Value Problems* (Cambridge University Press, Cambridge, 2008).

[8] K. D. Dorfman and H. Brenner, Phys. Rev. E **65**, 021103 (2002).

[9] P. M. Adler and J.-F. Thovert, *Fractures and Fracture Networks* (Kluwer Academic Publishers, Dordrecht, Netherlands, 1999).

[10] U. Hornung, *Homogenization and Porous Media* (Springer Verlag, NY, 1996).

[11] R. C. McPhedran, Proc. R. Soc. London, Ser. A **408**, 31 (1986).

[12] R. C. McPhedran and G. W. Milton, Proc. R. Soc. London, Ser. A **411**, 313 (1987).

[13] V. V. Mityushev and S. V. Rogosin, *Constructive Methods for Linear and Non-Linear Boundary Value Problems for Analytic Function. Theory and Applications* (Chapman & Hall/CRC, Monographs and Surveys in Pure and Applied Mathematics, Boca Raton, etc., 1999).

[14] V. Mityushev and P. Adler, ZAMM **82**, 335 (2002).

[15] V. Mityushev and P. Adler, ZAMP **53**, 486 (2002).

[16] V. Mityushev, J. Appl. Funct. Anal. **2**, 115 (2007).

[17] G. W. Milton, *The Theory of Composites* (Cambridge University Press, Cambridge, 2002).

[18] V. V. Jikov, S. M. Kozlov, and O. A. Oleinik, *Homogenization of Differential Operators and Integral Functionals* (Springer-Verlag, Berlin, 1994).

[19] S. Sisavath, V. V. Mourzenko, P. Genthon, J.-F. Thovert, and P. M. Adler, Geophys. J. Int. **157**, 917 (2004).

[20] D. J. Bergman, *Bulk Physical Properties of Composite Media*, Les Méthodes de l'homogénéisation: theorie et applications en physique (Eyrolles, Paris, 1985), pp. 1–128.

[21] A. N. Tikhonov and A. A. Samarskij, *Equations of Mathematical Physics* (Dover, New York, 1990).